

Effect of the strong metal-support interaction on hydrogen sorption kinetics of Pd-capped switchable mirrors

A. Borgschulte,* R. J. Westerwaal, J. H. Rector, B. Dam, and R. Griessen

Faculty of Sciences, Department of Physics and Astronomy, Vrije Universiteit De Boelelaan 1081, 1081 HV Amsterdam, The Netherlands

J. Schoenes

Institut für Halbleiterphysik und Optik, TU Braunschweig Mendelssohnstrasse 3, D-38106 Braunschweig, Germany

(Received 18 December 2003; revised manuscript received 1 July 2004; published 27 October 2004)

The morphology and electronic structure of Pd clusters grown on oxidized yttrium surfaces are investigated by scanning tunneling microscopy and ultraviolet photoelectron spectroscopy. The hydrogen sorption mediated by the Pd clusters is determined from the optically monitored switching kinetics of the underlying yttrium film. A strong thickness dependence of the hydrogen uptake is found. The electronic structure of the as-grown Pd clusters depends only weakly on their size. Strong changes of the photoemission spectra are found after hydrogenation, in particular the oxide peak shifts and the Pd peaks vanish. Both phenomena are due to a strong metal-support interaction (SMSI) state, characterized by a complete encapsulation of the clusters by a reduced yttrium oxide layer. Scanning tunneling spectroscopy confirms the SMSI state of small Pd clusters after hydrogen exposure. The SMSI effect is less important with increasing Pd thickness. This explains the critical thickness for the catalyzed hydrogen uptake by the Pd/YO_x/Y system. The results shed light on the mechanism of hydrogen absorption at the triple point gas-catalyst-oxide, which also plays an important role in today's fuel cell technology.

DOI: 10.1103/PhysRevB.70.155414

PACS number(s): 68.47.Jn

I. INTRODUCTION

Supported metal clusters are frequently applied as catalysts. Beside their use in gasoline octane improvement and automotive exhaust purification,¹ they may become a key ingredient for a sustainable hydrogen technology.² One specific example is the hydrogen storage in metal hydrides. For a fast hydrogen uptake kinetics, catalytic additives are used in such hydrogen storage systems.^{3,4} The reason is that nearly all hydride forming metals will be covered with an oxide skin, if stored in air or exposed to technical hydrogen with contaminants. This layer impedes hydrogen absorption.⁵⁻⁷ The additives consist of small particles which stick to the surface of the storage material and catalytically enhance the hydrogen uptake.⁸

The use of catalytic metal clusters was also successfully implemented in switchable mirrors by depositing a thin Pd capping layer on top of the optically active metal hydride.⁹ Several groups found that the switching kinetics—and consequently the hydrogen uptake rate—is mainly determined by the thickness of the catalytic Pd cap layer.^{10,11} In particular, it was observed that a minimum Pd thickness is required for a sufficient hydrogen uptake, an effect that remained unexplained until now.

However, already in the eighties, the morphology dependence of the catalytic activity of supported metal clusters in heterogeneous catalysis has been attributed to a so-called strong metal-support interaction (SMSI), characterized by an encapsulation of the clusters with material from the support.^{13,14} Moreover, it was found that the suppression of hydrogen chemisorption is a simple test for the SMSI state. We demonstrate here that the SMSI state of the deposited Pd

clusters is also the physical origin of the thickness dependence of the hydrogen uptake of switchable mirrors.¹⁵ The same effect is also expected to play a role in hydrogen storage (e.g., oxide catalysts on metal hydrides),³ fuel cells (catalytic metal clusters as part of the electrodes)¹⁶ and in related gasochromic devices made of WO₃.¹⁷

We investigate the morphology and the electronic structure of Pd clusters grown on oxidized yttrium surfaces, both as deposited and after hydrogenation. We have chosen to study Pd clusters on oxidized yttrium surfaces since their preparation is well known.^{6,9,10,18,19} Furthermore, the YH_x system can be considered as the archetypal switchable mirror material. Sample preparation and characterization are performed *in situ*. The electronic structure is determined by ultraviolet photoelectron spectroscopy (UPS). A strong change is observed in the spectra for small Pd thicknesses after hydrogen exposure, which is in contrast with existing photoemission data on hydrogenated bulk Pd.¹² The new states are explained in terms of a thin oxide layer, that encapsulates Pd clusters after hydrogenation, the characteristics of the SMSI state. As photoemission has no lateral resolution and depth profiling is difficult due to the cluster geometry, scanning tunneling microscopy (STM) and spectroscopy (STS) are used to confirm the SMSI state of Pd clusters. To link the measured electronic and geometric structures with the hydrogen-uptake kinetics, the switching kinetics of a Pd-capped surface-oxidized yttrium film is studied. The kinetics of such a sample with various Pd thicknesses is determined optically from the time dependence of the optical changes induced by H absorption in yttrium, i.e., the yttrium film is used as an indicator for the H concentration (see Ref. 20). This allows for an estimate of the catalytic activity of Pd

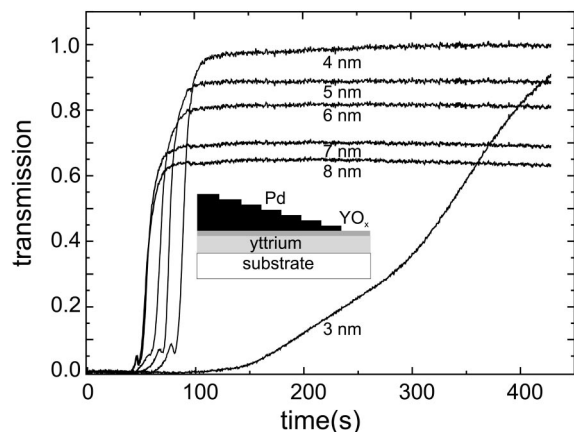


FIG. 1. Normalized optical transmission of a 200 nm thick yttrium film during loading in 1 bar hydrogen at room temperature. The Pd thickness ranges from 2 to 8 nm in steps of 1 nm (the sample setup is not on scale). The curves are arbitrarily normalized to the asymptotic value of the 4 nm sample. The time delay between the opening of the H valve and the maximum slope of the transmission-time function (due to the formation of the trihydride phase) is defined as the switching time of the film. The small peak is due to the infrared transparency window of the YH_2 phase.²¹

clusters. We show that the critical layer thickness for a catalytic activity of a Pd caplayer is due to the SMSI state of Pd on YO_x/Y .

II. EXPERIMENT

Epitaxial and polycrystalline Y is grown under ultrahigh vacuum (UHV) conditions in a metal-molecular beam epitaxy system with a base pressure of less than 2×10^{-10} mbar on $\text{CaF}_2(111)$ and amorphous quartz, respectively, using an electron (e)-gun evaporator. The pressure during evaporation remains below 1×10^{-9} mbar. The deposition rate (≈ 0.1 nm/s) is controlled by a quartz-crystal oscillator. The uncertainty of the layer thickness measured by the quartz oscillator is $\approx 10\%$. The substrate temperature during epitaxial (polycrystalline) yttrium growth is 700°C (room temperature). The freshly grown yttrium films are subsequently exposed to 10^{-6} mbar oxygen for 15 min to prepare a smooth oxide film on top of the yttrium.

For STM measurements the samples are transported in air to the STM chamber and immediately built in. The Pd is deposited *in situ* at room temperature using a mini-e-gun evaporator. STM images are taken with an Omicron UHV scanning probe microscope in constant current mode for the topography images and constant height mode for current imaging. The setup is adapted to withstand hydrogen up to one bar. The STM data are collected using an electrochemically etched tungsten tip.

Loading kinetics and photoemission measurements are performed on stepped samples with various Pd thickness on an oxidized polycrystalline yttrium film on quartz. The sample geometry is sketched in Fig. 1. For these measurements Pd is deposited directly after the oxidation process in the growth chamber. On one sample, a Pd stair consisting of

regions with increasing thickness is obtained by moving stepwise a shutter in one direction directly below the sample during evaporation. The samples are transported in UHV to the analysis chamber, which is equipped with an electron spectrometer. The cleanliness and the surface composition of the films are determined by Auger electron spectroscopy (AES). Photoemission measurements are performed with a He discharge lamp exciting the He I resonance line ($\hbar\omega = 21.2$ eV) and a hemispherical analyzer with a mean radius of 97 mm (Specs). The total energy resolution is about 100 meV, and the angular resolution is $\pm 5^\circ$. The measurements are carried out at room temperature. We emphasize here, that the spectra are always recorded under UHV conditions.

The hydrogen loading behavior of a stepped sample is monitored by exposing the whole sample to 1 bar of hydrogen gas in an optical microscope (Leitz). A charge coupled device camera and a personal computer are used to sequentially capture images. The manual H_2 gas loading introduces an overall uncertainty in the absolute switching time (≈ 2 s). Differences in kinetics for various Pd thicknesses can be measured accurately with a time resolution of about 0.1 s.

III. RESULTS

Due to the complexity of surface processes, several experimental techniques are needed to link the hydrogen-uptake kinetics to the morphology and the electronic properties of the cap layer of a switchable mirror. The optically measured hydrogen uptake kinetics as a function of the Pd cap layer thickness is discussed in Sec. III A. The observed extraordinary thickness dependence calls for an investigation of the electronic structure of the cap layer. Hence, we measure the electronic properties of a similar step sample by means of photoemission in Sec. III B. It is known from literature that an oxidized yttrium film is not fully covered with Pd for small thicknesses due to a clustering of the Pd.¹⁰ As a result, a detailed investigation of the morphology and its influence on the physical properties of the surface is needed. We discuss the morphology of the Pd cap layer measured by STM in Sec. III C. Since in photoemission, the size dependence of the electronic structure can only be measured for an area averaged thickness of the clustered surface, STS is used to confirm the UPS measurements of the electronic structure on a microscopic scale (Sec. III C).

A. Hydrogen uptake kinetics

The yttrium-hydrogen system exhibits three thermodynamic phases. The structural phase transitions are accompanied by changes in the electronic structure, which are affecting the optical properties of the material. Pure yttrium is a shiny metal. The dihydride YH_2 is also metallic, but has a weak transparency at a photon energy around 1.9 eV. YH_3 is an insulator with a band gap of 2.66 eV.²¹ As a result, a 200 nm thick YH_x film exhibits essentially zero transmission at low H concentrations, a very weak transmission in the red part of the visible spectrum for $x \approx 2$ (dihydride) and a large,

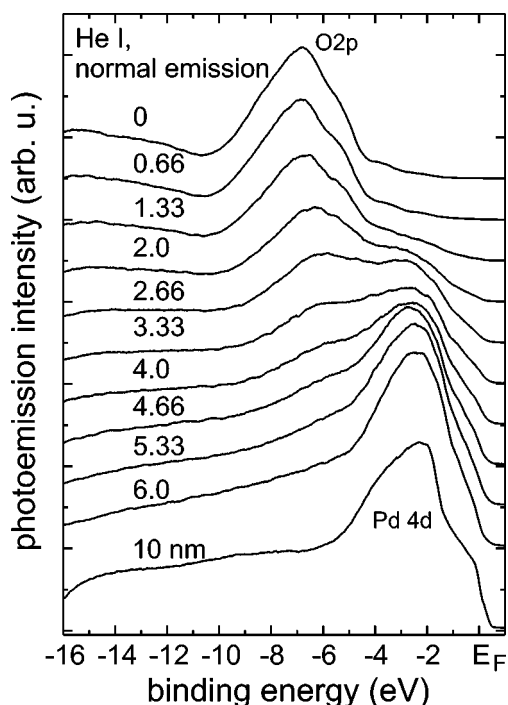


FIG. 2. Photoemission spectra of Pd covered surface-oxidized polycrystalline yttrium films (as grown). The nominal thickness of the Pd caplayer varies from 0 up to 10 nm.

yellowish transparency in the fully hydrogenated state $x \approx 3$ (trihydride). Thus, the optical transmission of a YH_x film provides a direct indication of the amount of hydrogen in the yttrium film.

Figure 1 shows the time dependence of the optical transmission of a surface oxidized, 200 nm thick yttrium film capped with Pd layers of various thicknesses during hydrogen loading. The time between the opening of the H_2 valve and the maximum slope of the transmission-time function (corresponding to the formation of the trihydride phase) is defined as the switching time of the film. The switching time depends strongly on the thickness of the Pd cap layer. It has a minimum at about 8 nm Pd and increases drastically for smaller thicknesses.¹⁰ Films covered with less than 3 nm Pd do not switch at all. This critical thickness depends slightly on the underlying yttrium surface. Pd evaporation on a clean yttrium surface in UHV results in a larger critical thickness.¹⁰ Smaller values than shown here can be obtained by growing an intermediate Al_2O_3 layer before depositing Pd.¹¹

B. Photoemission experiments

To relate the thickness dependence of the hydrogen uptake rate to the electronic structure of the surface, we performed photoemission studies on similar stepped films.

Figure 2 shows the development of the photoemission spectra of Pd on YO_x/Y for Pd thicknesses between 1 and 10 nm. The extraordinary changes in the hydrogen uptake kinetics described earlier take place in this thickness regime (compare Fig. 1). The energy distribution curves are taken at normal emission with a photon energy of 21.2 eV and are shifted for clarity with a constant value with respect to each

other. The binding energy is referred to the Fermi edge (E_F) of the 6 nm metallic Pd film. The features in the binding energy range 5–12 eV are valence bands of the underlying yttrium oxide film, comprising mainly O 2p states (the yttrium states are nearly empty and their photoionization probability is very low).²² Valence band transitions due to the Pd 4d electrons are between 0 and –4 eV,²³ where the emission from the yttrium oxide is weak and featureless.

The intensity of the O 2p peak decreases and that of the Pd 4d peak increases with increasing Pd thickness. This behavior of the photoemission intensity is to be expected from a decreasing Pd coverage at small thickness. Electronic effects are only expected from thicknesses below 1–2 Pd monolayers (corresponding to 0.3–0.5 nm), where a metal-insulator transition (MIT) has been observed in Pd clusters.^{24,25} Indeed, we find that spectra for 0.66 nm Pd show a finite photoemission intensity at the Fermi energy, smaller thicknesses were not studied here. Note, that the thickness reported for the MIT does not correspond to the critical thickness (3 nm), where we find that the hydrogen uptake increases markedly. Moreover, we do not observe striking differences between the 2.66 nm spectrum and the 3.33 nm spectrum (Fig. 2), which could shed light on the origin of the peculiarity of the critical thickness of 3 nm.

According to the literature¹⁰ and our own AES measurements,²⁶ surface-oxidized yttrium is totally covered for Pd thicknesses larger than 8 nm. Therefore, the 10 nm spectrum can be regarded as the bulk Pd spectrum. The asymmetric valence band is a result of the unresolved contribution of e_g and t_{2g} 4d bands in these polycrystalline films, while single-crystalline surfaces show a double peak structure.^{23,26} The absence of this asymmetry for smaller thickness arises therefore from their low crystallinity as determined by reflection high-energy electron diffraction²⁷ and the resulting underdeveloped band structure. This is in good agreement with measurements of Cini *et al.*²⁸ and Boyet *et al.*²⁹ (Pd on graphite) and Cai *et al.* (Pd on Al_2O_3).²⁴ The center of gravity of the 4d peak (–2.5 eV) remains nearly unchanged. This is evidence that there is no strong hybridization of the Pd states with the Y states. A strong hybridization due to alloy formation would be observed if the Pd were grown directly on a clean yttrium surface.^{27,30}

To explore the relation between hydrogen absorption and electronic structure, photoemission spectra are taken after exposure of the films to 1800 L hydrogen (1 L = 10^{-6} Torr·s).

The results are shown in Fig. 3. Hydrogenation leads to drastic changes in the spectra of especially the small clusters. In earlier photoemission experiments on hydrogenated *bulk* Pd no such strong changes of the photoemission spectra after hydrogen exposure were reported.¹² Indeed, the 10 nm spectrum in Fig. 3 does not show strong deviations after hydrogenation, evidencing that a 10 nm thick Pd layer behaves bulk-like. In particular, the additional peak at around –7.8 eV can be attributed to the hydrogen split-off state, in good agreement with theoretical³¹ and experimental values.³² These surface states are indicated in Fig. 3, $E(\bar{\Gamma}) = -7.9$ eV with a dispersion of about 2 eV up to $E(\bar{K}) = -5.9$ eV for the Pd (111) surface. Also the slightly changed form of the d states at –3 eV originates from hydrogen derived states according to Eberhardt *et al.*³³

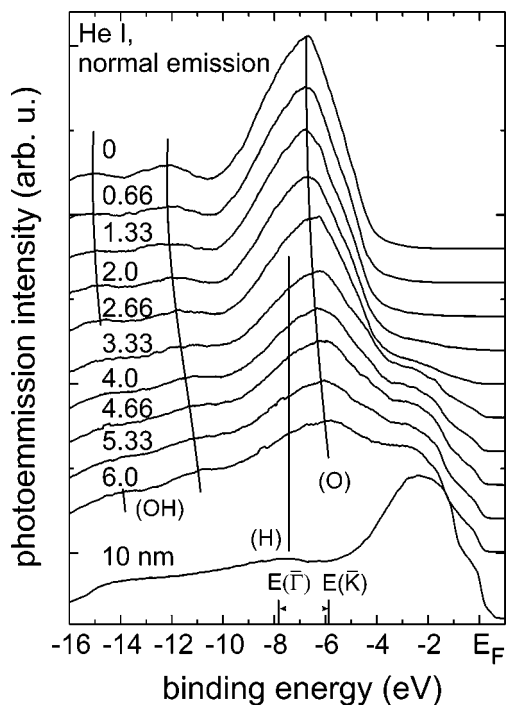


FIG. 3. Photoemission spectra of Pd covered polycrystalline yttrium films taken in UHV after exposure to 1800 L H₂. (OH) and (O) are attributed to yttrium hydroxide and oxide states, respectively. $E(\bar{\Gamma})$, $E(\bar{K})$ indicate the energies of the hydrogen induced split-off states on Pd(111).³³

Photoemission spectra of *thinner* Pd layers show a O $2p$ state peak around -6.5 eV (peak O in Fig. 4), which shifts with increasing thickness from -6.8 to -5.8 eV. Its intensity is much higher than the Pd- $4d$ states around -2.5 eV, which are strongly reduced compared to the as-grown spectra of identical thickness. Even the pure YO_x surface shows additional peaks after hydrogenation at around -12 and -14 eV, attributed to OH groups on the oxide surface.³⁴ This is a hint for an interaction of hydrogen with the YO_x surface. The interaction is altered by the presence of Pd (shift of the OH peak of $+1$ eV with increasing Pd thickness), while the binding energy of Pd- d states stays nearly constant. Both phenomena can be explained, if one assumes a migration of the hydrogenated oxide onto the clusters, identical to the geometrical explanation of the SMSI state.¹⁴ Accordingly, the photoemission intensity of the Pd is much smaller after hydrogenation, since UPS is a very surface sensitive measurements (less than 3 ML). At the same time oxide- and hydroxide states with slightly different binding energies hint to an interaction of the oxide with hydrogen. In other words: small Pd clusters are encapsulated by a reduced (hydrogenated) oxide, which is mobilized by the presence of hydrogen. Thus the catalytically active surface of the clusters is covered and their catalytic effect eliminated.

To follow the degree of coverage quantitatively, we plot the intensity at the Fermi level $I(E_F)$ as a function of the Pd thickness in Fig. 4(b). As expected, there is a sigmoidal evolution of $I(E_F)$ as a function of the thickness originating from an increasing Pd coverage of the YO_x surface for small effective thickness followed by a complete Pd coverage. This

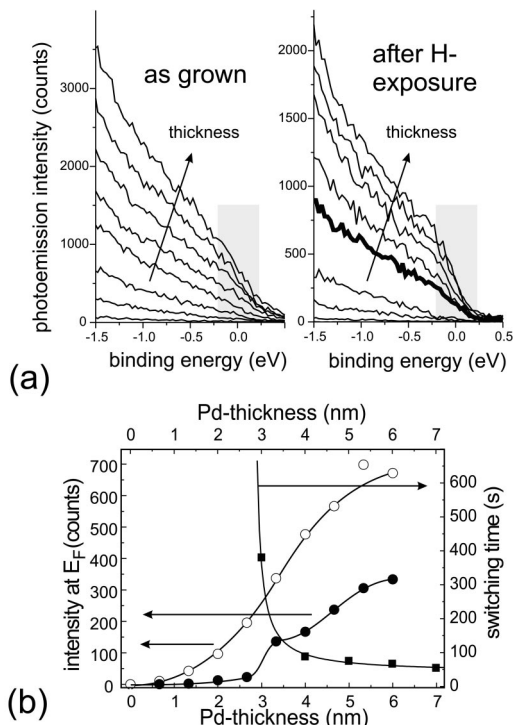


FIG. 4. (a) Details of the photoemission spectra of Figs. 2 (left) and 3 (right) near the Fermi edge. The spectra zero and 0.66 nm Pd are omitted for clarity. The thermal and spectrometer resolution broadening of the Fermi edge is indicated by the grey area. (b) The intensity at E_F for the as-deposited clusters increases smoothly (open circles), while there is a remarkable jump at 3 nm for the hydrogen exposed clusters (filled circles). The corresponding spectrum at the strong increase of $I(E_F)$ is plotted with a thick line in (a). For comparison the switching times taken from Fig. 1 are also plotted (squares; right scale). The lines are a guide to the eyes.

behavior is confirmed by following the evolution of the Pd $-d$ state photoemission intensity or using Auger electron spectroscopy. However, the latter method is problematic, since AES probes deeper than the surface [mean free path at 510 eV (O KLL line) is ≈ 1 nm]. Therefore one might use $I(E_F)$ as a measure of the free Pd surface. While only a smooth increase in the intensity as a function of thickness is found for the as-grown surfaces, a remarkable jump is seen for the hydrogen exposed Pd clusters. Here, $I(E_F)$ is nearly zero up to a thickness of 2.66 nm, resulting from nearly completely oxide covered Pd clusters. The sudden rise in intensity $I(E_F)$ around 3 nm evidences the evolution of uncovered Pd surfaces. For smaller thicknesses the clusters are buried under the hydrogenated oxide. Evidently the Pd thickness at the intensity jump coincides with the critical thickness needed for hydrogen absorption (see Fig. 4), which nicely confirms the SMSI state for small thicknesses.

C. SMSI state evidenced by STM

The morphology of Pd capped preoxidized polycrystalline yttrium films has been studied by several groups.^{10,27} In general, a polycrystalline film on quartz consists of yttrium

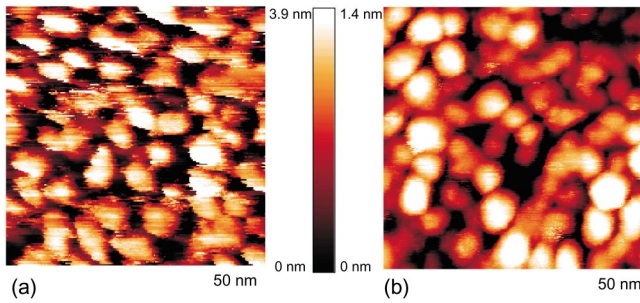


FIG. 5. Topography images of Pd clusters on Y(0001) on CaF_2 (111), directly after growth (a) and after exposure to 10^{-4} mbar hydrogen for 1 h (b), acquired at $U_{\text{gap}}=5$ V, $I=0.5$ nA and $U_{\text{gap}}=1$ V, $I=0.5$ nA, respectively. The nominal Pd thickness is 3 nm.

grains with a size between 50 and 400 nm for film thicknesses between 20 and 500 nm. The Y(-O) surface is covered by Pd clusters, typically 5–10 nm in diameter. Unfortunately, the roughness of the surface in combination with the limited tip radius of the STM makes it impossible to investigate the microscopic structure of Pd clusters in detail. Therefore, we concentrate on the investigation of Pd clusters on epitaxial yttrium films. Here, a surfactant assisted growth results in nearly atomically flat epitaxial Y(0001) layers on CaF_2 (111).^{18,19,35}

Due to the flatness of the epitaxial yttrium film, it is a perfect model system for the study of Pd clusters on top of a switchable mirror. A representative topography image of 3 nm Pd on top of a surface-oxidized 100 nm thick yttrium film is shown in Fig. 5(a). The film consists of nonconnected Pd clusters with an average diameter of 4 nm. Their height is about 3 nm as determined by height profiles. This value may be uncertain as the apparent height of surface structures strongly depends on their underlying electronic structure, in particular for oxide/metal structures (Hansen *et al.*).³⁶ The authors report an apparent height change of 25% for 2 nm Pd clusters on Al_2O_3 in the bias interval from 1 to 4 V. The 25% value may therefore be taken as the error bar of our measurements. Additional errors might arise from the circumstance that the STM tip sometimes moves the clusters, because the adhesion (interaction) of Pd with the underlying yttrium oxide is very small. This explains the bad quality of the image even at high bias voltages (“stripes” in the image).

However, high-quality images are obtained after hydrogen exposure of 10^{-4} mbar for 1 h [Fig. 5(b)]. This is a first hint that the interaction between Pd and YO_x is drastically strengthened, since images can be taken now without moving clusters. A second hint is the reduced maximum height of the clusters (1.5 nm, this result is independent of the bias voltage within 10%).

The effect of hydriding on the structure of thin metal films has been the subject of a number of investigations (see, e.g., Ref. 37, and references therein). A simple mechanism for the hydrogenation effect on Pd clusters was proposed by Dankert and Pundt. They consider only the “bulking” of the islands due to the hydrogen induced lattice expansion of each cluster.³⁸ As a consequence, the total electric resistance of the film drops drastically. To account for this effect Dankert and Pundt³⁸ assume that the Pd islands are near the percola-

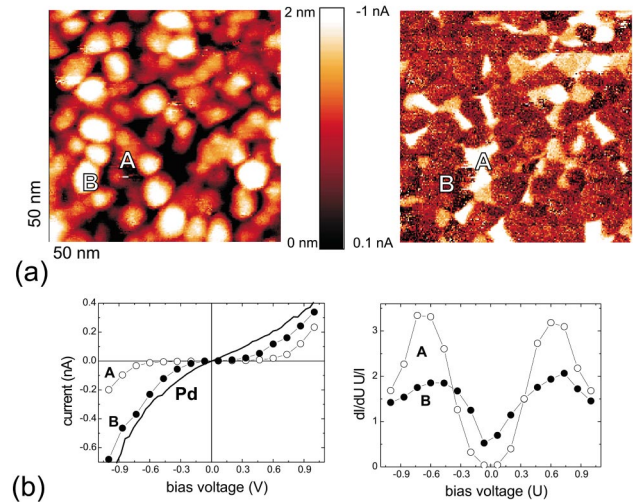


FIG. 6. (a) Topography (left, $U_{\text{bias}}=+1$ V) and current image (right, $U_{\text{bias}}=-1$ V) of 3 nm Pd clusters after exposure to 10^{-4} mbar of hydrogen, image size 50×50 nm². The different I - U curves correspond to different electronic structures. This is explicitly illustrated at the two points A and B in (b). The left panel shows the as-measured I - U curves, the right one the calculated DOS $= (dI/dU)(U/T)$. For comparison the I - U curves for a 10 nm thick Pd layer is included.

tion limit and become connected due to a linear increase of the lattice parameter (isotropic change).³⁹ On the other hand, the corresponding maximal change of +4.4% is relatively small, assuming a maximum hydrogen concentration of $\Delta x = 0.7$ in PdH_x . However, we observe a flattening of the islands. This contrast is understood if one considers the SMSI state, i.e., an interaction of hydrogen with the oxide near a cluster, which (i) changes the conductivity of the oxide (hydrogen acts as a donor in the oxide)⁴⁰ and (ii) buries the Pd clusters in it.

To find further evidence for this scenario we measure the local surface electronic structure of the clusters, since oxide covered clusters should display a different electronic structure than clean Pd clusters. For this, the measurements of local I - U curves at constant tip-sample distance are extended to every pixel in an image [current imaging tunneling spectroscopy (CITS)] to map the electronic structure of the surface. This gives us an insight into the size dependence of the electronic structure of the Pd clusters. Figure 6(a) compares the topography image with the corresponding current image at -1 V for a nominal Pd thickness of 3 nm. The CITS image displays low and high current regions. The areas correlate roughly with the island structure shown in the topography image (Fig. 6).

To determine the surface density of states (DOS) the tunneling current at various bias voltages is measured [Fig. 6(b)]. From the derivative of the I - U dependence the DOS can be estimated, following the simple expression for tunneling:

$$I \propto \int_0^{eU} n_t(\pm eU \mp E) \cdot n_s(E) \cdot T(E, eU) dE,$$

where n_t and n_s are the DOS of the tip and the surface, respectively, and $T(E, eU)$ is the tunneling transmission

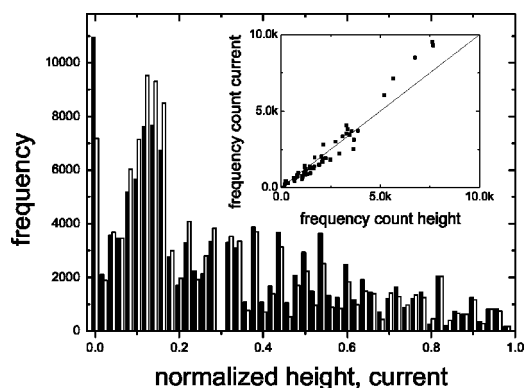


FIG. 7. Frequency of height—(black columns) and current—(white columns) amplitudes from Fig. 6. The amplitudes are normalized to maximum height. The frequency counts are compared to each other to demonstrate the correlation.

function.⁴¹ With $dn_t/dU \approx 0$ and $dT/dU \approx 0$ the first derivative

$$\frac{dI}{dU}(U) \propto en_t(U) \cdot n_s(eU) \cdot T(eU) \quad (1)$$

is proportional to the density of states of the surface.

The thus estimated DOS is plotted as a function of the bias voltage (equals binding energy) in Fig. 6(b) for two representative points (A, B). From these measurements we conclude that white areas (A) in Fig. 6 are oxides, since a clear gap in the DOS is detected. Darker areas (B) are metallic, i.e., with a finite DOS at E_F (=zero bias voltage). A qualitative comparison between topography and electronic structure suggests that small clusters and the borders of large clusters are covered by oxides (hydroxides). However, a direct comparison between height amplitudes and current amplitudes is difficult, because the measured height depends both on the Pd-clusters height and on the underlying structure.

To underline the correlation, the height and current distributions of the corresponding images in Fig. 6 are given in Fig. 7. Considering the frequencies instead of comparing height and current directly has the advantage that long-range fluctuations are eliminated. Indeed, the frequencies of both properties scale with each other. The frequency counts of a given height and current, respectively, are compared in the inset of Fig 7. The 1:1 correspondence demonstrates a clear correlation between the cluster height its electronic structure, i.e., the thickness behavior of the SMSI state. Further evidence for the thickness dependence of the SMSI state is that thick (>8 nm) films have a uniform appearance in CITS images (not shown).

IV. DISCUSSION

The physics of hydrogen absorption in metals is strongly related to heterogenous catalysis on surfaces as in both cases, the crucial step of the involved processes is the chemisorption and dissociation of the gas(es) on the metal surface.^{5,42} Therefore many ideas and results obtained from catalysis re-

search can be used to explain hydrogen absorption. In particular, the switching kinetics of a switchable mirror may be seen primarily as a measure for the catalytic activity of its surface. Thus, we attribute the strongly reduced hydrogen uptake rate at low Pd coverage to a catalytically inactivated Pd surface (Fig. 1).

It is well known that clusters can behave differently than bulk materials.^{1,43} Therefore, one might attribute the critical Pd thickness for hydrogen absorption to a reduced catalytic activity of small Pd clusters (Sec. III A). However, the photoemission experiments presented in this publication do not show a substantial thickness effect of the electronic structure of as-grown clusters. Accordingly, one has to conclude that the catalytic properties of small Pd clusters are intrinsically not very different from that of larger ones. This is underlined by the observation that already the thinnest Pd layers on surface-oxidized yttrium show changes in the photoemission spectra after hydrogenation, i.e., an interaction of the thin-film system with hydrogen has taken place. The Pd states vanish, but do not change in energy (Sec. III B). In addition, we find hard evidence for an interaction of hydrogen with the yttrium oxide. In principle, a reaction of the pure oxide with hydrogen is possible (yttrium hydroxide is more stable than yttrium oxide),⁴⁴ but usually it is kinetically hindered. Moreover, also hydrogenated yttrium oxide surfaces are still catalytically inactive. This point is clearly evidenced by the fact that surface-oxidized yttrium films without a Pd cplayer do not absorb hydrogen. Dissociative hydrogen adsorption and the subsequent diffusion through the underlying oxide, only takes place via the Pd clusters. Accordingly, yttrium oxide interacts with hydrogen, which has been split by Pd clusters. The interaction with hydrogen includes the rearrangement of atoms, therefore it is likely that YO_x becomes more mobile allowing the system to reach its thermodynamical equilibrium, which is not the as-grown state. The latter is recognized by the observation that Pd grows in an island mode. This is due to the fact, that the surface energy of Pd is larger than the sum of the surface energy of the yttrium oxide plus the interface energy between Pd and the oxide.^{45,46} Lowering the surface energy stabilizes the system. Consequently, an encapsulation of Pd clusters by a yttrium hydroxide with a small surface energy is thermodynamically favored. This encapsulation is called SMSI.^{13,14} However, the required diffusion path length for the yttrium and oxygen atoms increases with increasing cluster size. Thus, a full encapsulation is only observed for small clusters as sketched in Fig. 8. Larger clusters can still absorb hydrogen, since they are not fully encapsulated. This scenario is in full agreement with the observed switching times (Fig. 1). The minimum thickness for hydrogen absorption corresponds to the first appearance of free Pd surfaces (photoemission experiments, Fig. 4), the minimum switching time (fastest kinetics) corresponds to a fully Pd-covered surface.

To illustrate the scenario, the transmission image of a Pd-wedge sample is included in Fig. 8. The sample is first loaded in 1 bar hydrogen at room temperature and stored in air for several hours. After hydrogen exposure *small* clusters are fully encapsulated by a reduced (hydrogenated) yttrium oxide (hydroxide) that blocks hydrogen uptake. Thus the corresponding region shows no transmission (region III).

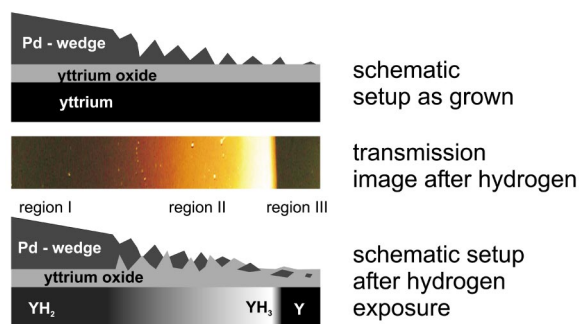


FIG. 8. SMSI effect as a function of thickness for Pd on oxidized yttrium. The top shows the schematic setup of the thin film system, the bottom the resulting SMSI effect. The middle shows a transmission image after hydrogen exposure and subsequent unloading in air of such a thin film. After hydrogen exposure small clusters are fully encapsulated by a reduced (hydrogenated) yttrium oxide (region III). Still, some have enough free surface to load the yttrium film up to the trihydride phase, while an unloading is not longer possible (region II). A coalesced layer switches reversibly (region I).

Thicker clusters have at the beginning enough free metal surface to load the yttrium film up to the trihydride phase (region II). However, an unloading (the reversed process) is not possible any longer, since the clusters are fully encapsulated in the meantime during the loading process. Therefore, the film covered with these clusters remains in the fully loaded state, as nicely visible in region II (Fig. 8). This SMSI effect might also be responsible for the degradation of switchable mirrors, which is observed more or less in all material systems.⁴⁷ A closed Pd film will extend the SMSI-free time period (region I), but might not eventually prevent it. On the other hand, it was reported that the SMSI effect depends on the amount of contaminations in the hydrogen gas and might be reversed by exposing the sample to oxygen.^{13,48} Indeed, it was found that the unloading kinetics of switchable mirrors can be enhanced by exposing them to air or oxygen.⁴⁹

V. CONCLUSIONS

The morphology and electronic structure of Pd clusters grown on oxidized yttrium surfaces are investigated by scanning tunneling microscopy and ultraviolet photoelectron spectroscopy. The hydrogen sorption mediated by the Pd clusters is determined by the optically monitored switching kinetics of the underlying yttrium film. A strong thickness dependence of the hydrogen uptake is found. The electronic structure of the as grown Pd clusters shows only a minor dependence on their size. However, strong changes of the photoemission spectra are found after hydrogenation, in particular the oxide peak shifts and the Pd peaks vanish. Both phenomena are explained by the SMSI state, characterized by an encapsulation of the clusters by a reduced yttrium oxide (hydroxide) layer. Thus the catalytically active surface of the Pd clusters is covered and their catalytic effect eliminated. The thickness effect of the hydrogen absorption corresponds to the thickness dependence of the amount of free Pd surface as determined by photoemission. The degree of encapsulation decreases with increasing Pd thickness. Small clusters are completely covered with the yttrium oxide (-hydroxide), which explains the minimum thickness required for a fast hydrogen-uptake kinetics. The SMSI state of small clusters is confirmed by scanning tunneling spectroscopy on microscopic scale. The results point towards the understanding of hydrogen absorption in metals, which is the crucial step in all applications involving hydrogen sorption in fuel cells, metal-hydrides and switchable mirrors. The correlation between electronic structure and catalytic activity can be used to enhance the efficiency of catalysts and is therefore of vital importance to the hydrogen energy technology.

ACKNOWLEDGMENTS

The authors are very grateful to Dr. W. Lohstroh for stimulating discussions. This work is financially supported by the Stichting voor Fundamenteel Onderzoek der Materie (FOM) and the Nederlandse Organisatie voor Wetenschappelijk Onderzoek (NWO) through the ACTS program.

*Electronic address: borg@nat.vu.nl

¹H. J. Freund, Surf. Sci. **500**, 271 (2002).

²L. Schlapbach and A. Züttel, Nature (London) **414**, 353 (2001).

³G. Barkhordarian, T. Klassen, and Rüdiger Bormann, Scr. Mater. **49**, 213 (2003).

⁴J. F. Pelletier, J. Huot, M. Sutton, R. Schulz, A. R. Sandy, L. B. Lurio, and S. G. J. Mochrie, Phys. Rev. B **63**, 052103 (2001).

⁵L. Schlapbach, in *Hydrogen in Intermetallic Compounds II*, edited by L. Schlapbach (Springer-Verlag, Berlin, 1992).

⁶J. Hayoz *et al.*, J. Vac. Sci. Technol. A **18**, 2417 (2000). The authors reported the hydrogenation of epitaxial yttrium films without any protective layer up to the trihydride phase. They grew the yttrium layers in a very clean UHV environment (10^{-11} mbar) and exposed the films to *in situ* purified hydrogen.

⁷H. C. Siegmann, L. Schlapbach, and C. R. Brundle, Phys. Rev.

Lett. **40**, 972 (1978).

⁸E. Fromm and H. Uchida, J. Less-Common Met. **131**, 1 (1987).

⁹J. N. Huiberts, R. Griessen, J. H. Rector, R. J. Wijngaarden, J. P. Dekker, D. G. de Groot, and N. J. Koeman, Nature (London) **380**, 231 (1996).

¹⁰S. J. van der Molen, J. W. J. Kerssemakers, J. H. Rector, N. J. Koeman, B. Dam, and R. Griessen, J. Appl. Phys. **86**, 6107 (1999).

¹¹A. T. M. van Gogh, S. J. van der Molen, J. W. J. Kerssemakers, N. J. Koeman, and R. Griessen, Appl. Phys. Lett. **77**, 815 (2000).

¹²W. Eberhardt, F. Greuter, and E. W. Plummer, Phys. Rev. Lett. **46**, 1085 (1981).

¹³S. J. Tauster, S. C. Fung, R. T. K. Baker, and J. A. Horsely, Science **211**, 1121 (1981).

- ¹⁴O. Dulub, W. Hebenstreit, and U. Diebold, *Phys. Rev. Lett.* **84**, 3646 (2000).
- ¹⁵V. M. Belousov, M. A. Vasylyev, L. V. Lyashenko, N. Yu. Vilko, and B. E. Nieuwenhuys, *Chem. Eng. J.* **91**, 143 (2003).
- ¹⁶S. M. Haile, *Mater. Today* **6**, 24 (2003).
- ¹⁷A. Georg, W. Graf, D. Schweiger, V. Wittwer, P. Nitz, and H. R. Wilson, *Sol. Energy* **62**, 215 (1998).
- ¹⁸D. G. Nagengast, J. Kerssemakers, A. T. M. van Gogh, B. Dam, and R. Griessen, *Appl. Phys. Lett.* **75**, 1724 (1999).
- ¹⁹A. Borgschulte, S. Weber, and J. Schoenes, *Appl. Phys. Lett.* **82**, 2898 (2003).
- ²⁰A. Remhof, J. L. M. van Mechelen, N. J. Koeman, J. H. Rector, R. J. Wijngaarden, and R. Griessen, *Rev. Sci. Instrum.* **74**, 445 (2003); see also F. J. A. den Broeder *et al.*, *Nature (London)* **394**, 656 (1998).
- ²¹A. T. M. van Gogh, D. G. Nagengast, E. S. Kooij, N. J. Koeman, J. H. Rector, R. Griessen, C. F. J. Flipse, and R. J. J. G. A. M. Smeets, *Phys. Rev. B* **63**, 195105 (2001).
- ²²J. J. Yeh and I. Lindau, *At. Data Nucl. Data Tables* **32**, 1 (1985).
- ²³J. S. Kang, D. W. Hwang, C. G. Olson, S. J. Youn, K. C. Kang, and B. I. Min, *Phys. Rev. B* **56**, 10 605 (1997).
- ²⁴Y. Q. Cai, A. M. Bradshaw, Q. Guo, and D. W. Goodman, *Surf. Sci.* **399**, L357 (1998).
- ²⁵A. Sandell, J. Libuda, P. Brühwiler, S. Anderson, A. Maxwell, M. Bäumer, N. Mårtensson, and H. J. Freund, *J. Electron Spectrosc. Relat. Phenom.* **76**, 301 (1995).
- ²⁶A. Borgschulte, Thesis, TU Braunschweig, 2003, <http://www.biblio.tu-bs.de/ediss/data/20030217a/20030217a.html>
- ²⁷A. Borgschulte, M. Rode, A. Jacob, and J. Schoenes, *J. Appl. Phys.* **90**, 1147 (2001).
- ²⁸M. Cini, M. De Crescenzi, F. Patella, N. Motta, M. Sastry, F. Rochet, and C. Verdozzi, *Phys. Rev. B* **41**, 5685 (1990).
- ²⁹M. Bovet, E. Boschung, J. Hayoz, Th. Pillo, G. Dietler, and P. Aebi, *Surf. Sci.* **473**, 17 (2001).
- ³⁰G. Faraci, S. La Rosa, A. R. Pennisi, Y. Hwu, L. Lozzi, and G. Margaritondo, *J. Appl. Phys.* **73**, 749 (1993).
- ³¹W. Dong, G. Kresse, J. Kurthmüller, and J. Hafner, *Phys. Rev. B* **54**, 2157 (1996).
- ³²F. Greuter, I. Strathy, E. W. Plummer, and W. Eberhardt, *Phys. Rev. B* **33**, 736 (1986).
- ³³W. Eberhardt, S. G. Louie, and E. W. Plummer, *Phys. Rev. B* **28**, 465 (1983).
- ³⁴R. I. R. Blyth, C. Searle, N. Tucker, R. G. White, T. K. Johal, J. Thompson, and S. D. Barrett, *Phys. Rev. B* **68**, 205404 (2003).
- ³⁵J. Hayoz, J. Schoenes, L. Schlapbach, and P. Aebi, *J. Appl. Phys.* **90**, 3925 (2001).
- ³⁶K. H. Hansen, T. Worren, E. Laegsgaard, F. Besenbacher, and I. Steensgaard, *Surf. Sci.* **475**, 96 (2001).
- ³⁷C. T. Campbell, *Surf. Sci. Rep.* **27**, 1 (1997).
- ³⁸O. Dankert and A. Pundt, *Appl. Phys. Lett.* **81**, 1618 (2002).
- ³⁹B. Baranowski, S. Majchrzak, and T. B. Flanagan, *J. Phys. F: Met. Phys.* **1**, 258 (1971). Even the assumed maximal hydrogen concentration of 0.7 is unrealistic, as the value is only obtained at a pressure of about 10^5 Pa.
- ⁴⁰Y. Larring and T. Norby, *Solid State Ionics* **77**, 147 (1995).
- ⁴¹R. Wiesendanger, *Scanning Probe Microscopy and Spectroscopy* (Cambridge University Press, Cambridge, 1994).
- ⁴²V. F. Kiselev and O. V. Krylov, *Adsorption and Catalysis on Transition Metals and Their Oxides* (Springer-Verlag, Berlin, 1988).
- ⁴³A. Züttel, Ch. Nützenadel, G. Schmid, D. Chartouni, and L. Schlapbach, *J. Alloys Compd.* **293**, 472 (1999).
- ⁴⁴ $\Delta H(Y_2O_3) = -900$ kJ/mol Y; $\Delta H(Y(OH)_3) = -1400$ kJ/mol Y; from R. C. Weast and M. J. Astle, *CRC Handbook of Chemistry and Physics* (CRC, Boca Raton, FL, 1979), p. 77.
- ⁴⁵E. Bauer, *Z. Kristallogr.* **110**, 372 (1958); E. Bauer and H. Poppa, *Thin Solid Films* **12**, 167 (1972).
- ⁴⁶J. Y. Tsao, *Materials Fundamental of Molecular Beam Epitaxy* (Academic, Boston, 1992).
- ⁴⁷P. H. L. Notten, *Curr. Opin. Solid State Mater. Sci.* **4**, 5 (1999).
- ⁴⁸A. R. Gonzales-Elipe, P. Malet, J. P. Espinos, A. Caballero, and G. Munera, in *Structure and Reactivity of Surfaces*, edited by C. Morterra, A. Zecchina, and G. Costa, (1989), p. 427.
- ⁴⁹R. Griessen, B. Dam, and I. A. M. E. Giebels (unpublished).